



biblio.ugent.be

The UGent Institutional Repository is the electronic archiving and dissemination platform for all UGent research publications. Ghent University has implemented a mandate stipulating that all academic publications of UGent researchers should be deposited and archived in this repository. Except for items where current copyright restrictions apply, these papers are available in Open Access.

This item is the archived peer-reviewed author-version of: In-Line UV spectroscopy for the quantification of low-dose active ingredients during the manufacturing of pharmaceutical semi-solid and liquid formulations

Authors: Bostijn N., Hellings M., Van der Veen M., Vervaet C., De Beer T.

In: *Analytica Chimica Acta*, 1013: 54-62

To refer to or to cite this work, please use the citation to the published version:

Bostijn N., Hellings M., Van der Veen M., Vervaet C., De Beer T. (2018) In-Line UV spectroscopy for the quantification of low-dose active ingredients during the manufacturing of pharmaceutical semi-solid and liquid formulations

Analytica Chimica Acta, 1013: 54-62

DOI: [10.1016/j.aca.2018.02.007](https://doi.org/10.1016/j.aca.2018.02.007)

In-line UV spectroscopy for the quantification of low-dose active ingredients during the manufacturing of pharmaceutical semi-solid and liquid formulations

N. Bostijn ^a, M. Hellings ^b, M. Van Der Veen ^b, C. Vervaet ^c, T. De Beer ^{a,*}.

^a Laboratory of Pharmaceutical Process Analytical Technology, Ghent University, Ottergemsesteenweg 460, 9000 Ghent, Belgium

^b Johnson & Johnson Pharmaceutical Research and Development, Analytical Development, Turnhoutseweg 30, 2340 Beerse, Belgium

^c Laboratory of Pharmaceutical Technology, Ghent University, Ottergemsesteenweg 460, 9000 Ghent, Belgium

*Corresponding author: Thomas De Beer

Ghent University

Laboratory of Pharmaceutical Process Analytical Technology,

Ottergemsesteenweg 460

9000 Ghent (Belgium)

Tel. +32 9 264 80 97

Fax +32 9 222 82 36

E-mail: Thomas.DeBeer@UGent.be

1 **Abstract**

2 UltraViolet (UV) spectroscopy was evaluated as an innovative Process Analytical
3 Technology (PAT) - tool for the in-line and real-time quantitative determination of low-
4 dosed active pharmaceutical ingredients (APIs) in a semi-solid (gel) and a liquid
5 (suspension) pharmaceutical formulation during their batch production process. The
6 performance of this new PAT-tool (i.e., UV spectroscopy) was compared with an already
7 more established PAT-method based on Raman spectroscopy. In-line UV measurements
8 were carried out with an immersion probe while for the Raman measurements a non-
9 contact PhAT probe was used. For both studied formulations, an in-line API quantification
10 model was developed and validated per spectroscopic technique. The known API
11 concentrations (Y) were correlated with the corresponding in-line collected preprocessed
12 spectra (X) through a Partial Least Squares (PLS) regression. Each developed
13 quantification method was validated by calculating the accuracy profile on the basis of the
14 validation experiments. Furthermore, the measurement uncertainty was determined
15 based on the data generated for the determination of the accuracy profiles. From the
16 accuracy profile of the UV- and Raman-based quantification method for the gel, it was
17 concluded that at the target API concentration of 2 % (w/w), 95 out of 100 future routine
18 measurements given by the Raman method will not deviate more than 10 % (relative error)
19 from the true API concentration, whereas for the UV method the acceptance limits of 10
20 % were exceeded. For the liquid formulation, the Raman method was not able to quantify
21 the API in the low-dosed suspension (0.09 % (w/w) API). In contrast, the in-line UV method
22 was able to adequately quantify the API in the suspension. This study demonstrated that
23 UV spectroscopy can be adopted as a novel in-line PAT-technique for low-dose

24 quantification purposes in pharmaceutical processes. Important is that none of the two
25 spectroscopic techniques was superior to the other for both formulations: the Raman
26 method was more accurate in quantifying the API in the gel (2 % (w/w) API), while the UV
27 method performed better for API quantification in the suspension (0.09 % (w/w) API).

28 **Keywords**

29 In-line UV spectroscopy, In-line Raman spectroscopy, Semi-solids, Liquids, Process
30 Analytical Technology (PAT), Accuracy profile.

31 **1. INTRODUCTION**

32 Spectroscopic techniques are increasingly proposed as alternative methods for the
33 quantification of APIs in pharmaceuticals. This is due to their advantages over the
34 traditional techniques, such as fast, in-line, non-invasive and non-destructive
35 measurements without the need of sample preparation. Near infrared (NIR) and Raman
36 spectroscopy have been identified as effective PAT-tools for real-time measurements of
37 critical process and product attributes during pharmaceutical processing. Raman
38 spectroscopy is until now mostly applied for solid dosage forms [1]–[6]. Some in-line
39 quantitative applications for hot-melt extrusion processes have also been reported [7]–[9].
40 Raman spectroscopy has an added value for quantification purposes of pharmaceutical
41 formulations where water is present, such as in semi-solid and liquid formulations, since
42 water produces almost no Raman signal. Research has already been conducted to
43 investigate the opportunity offered by Raman spectroscopy for these formulations [10]–
44 [15], however less frequently as an in-line analytical tool [16]. For some applications, these
45 spectroscopic techniques are not feasible, such as those that require the quantification of

46 low-dosed analytes. Fluorescence spectroscopy can be an alternative to the conventional
47 spectroscopic techniques for these applications because of its high sensitivity and
48 detection sensitivity [17], [18]. A drawback of fluorescence spectroscopy is that the analyte
49 needs to be a native fluorophore in order to detect it, which limits the number of possible
50 applications for this technique [19].

51 UV spectroscopy is a widely used quantitative analytical technique that finds its
52 application in many research domains and is capable of quantifying very low
53 concentrations ($< 0.01\%$) [20]–[24]. Nevertheless, studies describing on-line and in-line
54 applications of UV/VIS spectroscopy with fibre-optic probes are limited. O’Keeffe et al.
55 monitored the ozone concentration of a gas in an aluminium glass cell with a fibre-based
56 UV/VIS spectroscopy system [25]. Quinn et al. followed the reaction of a nucleoside with
57 trityl chloride in pyridine in a liquid environment [26], using a fibre-optic transmission
58 probe. The concentration of starting material and product was predicted via a PLS
59 regression model. Furthermore, a mixing study using a fibre-optic UV/VIS monitoring
60 technique was reported by Ng and Assirelli [27]. In this paper, bromophenol blue sodium
61 salt was used as a non-reactive tracer in distilled water. A good agreement between the
62 UV/VIS technique and the traditional conductivity technique was found. Other examples
63 of on-line and in-line UV spectroscopic applications in literature are drug dissolution tests,
64 where the drug release was monitored in real-time [24], [28]. However, the use of UV
65 spectroscopy for in-line monitoring of critical quality attributes during pharmaceutical
66 manufacturing processes of semi-solids and liquids is not yet described in literature.

67 In this study, UV spectroscopy was evaluated as a new PAT-tool for the in-line and real-
68 time monitoring of the API concentration during the production of pharmaceutical semi-

69 solid and liquid formulations. Furthermore, the performance of this new PAT-tool was
70 compared with an already established and widely adopted PAT-method based on Raman
71 spectroscopy. The in-line UV spectroscopic measurements were carried out by an
72 immersion probe. For the in-line Raman measurements, a PhAT probe was used. This
73 type of Raman probe was until now only applied in pharmaceutical unit operations such
74 as milling, blending and coating of solid dosage forms [29]. A pharmaceutical gel and
75 suspension with an API concentration of 2 and 0.09 % (w/w), respectively, were selected
76 as model formulations. For both formulations, a PLS regression model was developed per
77 spectroscopic technique and the quantification abilities of both techniques were
78 compared. The validation of the calibration models was assessed via accuracy profiles, a
79 validation strategy for quantitative analytical procedures proposed by the Société
80 Francaise des Sciences et Techniques Pharmaceutiques (SFSTP) [30]–[32].

81 **2. MATERIALS AND METHODS**

82 **2.1. Materials**

83 Commercially available pharmaceutical formulations were kindly provided by Janssen
84 Pharmaceutica (Beerse, Belgium): a semi-solid (gel) and a liquid (suspension), having an
85 API target concentration of 2 % and 0.09 % (w/w), respectively. Laboratory-scale batches
86 of the formulations were manufactured based on confidential information provided by
87 Janssen Pharmaceutica.

88 **2.2. Methods**

89 ***2.2.1. Experimental setup***

90 All formulations were produced with a customized IKA LR2000 mixing system (IKA,
91 Staufen, Germany). The mixing vessel was equipped with a heated jacket for controlling
92 the temperature of the process using a water bath (Type 1032, GFL, Burgwedel,
93 Germany). Interface openings were provided in the cover of the mixing vessel for the
94 implementation of the UV and Raman probe (figure 1).

95 **2.2.2. Calibration and validation samples**

96 In total, one calibration batch and three validation batches were produced for each
97 formulation. Validation batch one and three were produced by operator A and validation
98 batch two by operator B. Also, the validation batches were produced on three different
99 days. Instead of producing a complete batch for each concentration level of the calibration
100 (80, 90, 95, 100, 105, 110 and 120 % relative to target) and validation (85, 95, 100, 105
101 and 115 % relative to target) set, all the concentration levels were created using one
102 calibration batch and three validation batches (three different days). This was done by the
103 stepwise addition of API to a batch, corresponding to the different concentration levels.
104 The calibration batch was produced following the standard batch production procedure of
105 the formulations. However, instead of producing a batch with the target API concentration
106 (i.e., 100 % of target), the calibration batch contained only 80 % of the target API
107 concentration. After completing batch manufacturing, spectra of the lowest concentration
108 level (i.e., 80 % of target) were collected in-line while the formulation was being mixed.
109 Next, a specific amount of API was added to the calibration batch, corresponding to the
110 subsequent concentration level (i.e., 90 % of target), followed by the collection of spectra.
111 These steps (i.e., API addition and spectra recording) were repeated until the highest
112 concentration level (i.e., 120 % of target) was reached for the calibration batch, and

113 spectra were recorded at each concentration. The validation batches were produced
114 following the same procedure as described for the calibration batch, but with other
115 concentration levels (85, 95, 100, 105 and 115 % relative to target). During this procedure
116 (i.e., API addition and spectra recording), the formulation was mixed with a constant
117 mixing speed.

118 **2.2.3. UV spectroscopy**

119 An Avaspec-ULS2048L spectrometer (Avantes, Apeldoorn, The Netherlands), equipped
120 with a CCD detector, was connected by a fibre-optic cable to an immersion probe with a
121 45 degree angle window. The probe contained six illumination fibres and one detection
122 fibre. The light source was an AvaLight Deuterium-Halogen Lamp. All spectra were
123 acquired in the 200 - 1100 nm spectral range. The exposure time was 1000 ms and 950
124 ms for the gel and suspension, respectively, with each spectrum the average of 5 scans
125 and a total of 40 spectra/concentration level. The immersion probe was inserted via the
126 cover of the mixing vessel through a custom made interface (figure 1b).

127 **2.2.4. Raman spectroscopy**

128 In-line Raman spectra were recorded using a Raman Rxn2 spectrometer (Kaiser Optical
129 Systems, Ann Arbor, MI, USA), equipped with a CCD detector and a fibre-optic PhAT
130 probe. The laser wavelength was 785 nm with a laser power of 400 mW. The spectral
131 range of the system was 150 - 1890 cm^{-1} with a resolution of 5 cm^{-1} . For all formulations
132 an exposure time of 15 s with no averaging was used and every 30 s a spectrum was
133 recorded. Per concentration level, 30 spectra were collected in-line for both the calibration
134 and validation sets. The Raman PhAT probe was implemented through an opening in the

135 cover of the mixing vessel and fixed with a sealing to ensure a fixed probe position (figure
136 1c).

137 **2.2.5. Development of the calibration models**

138 For each formulation one calibration model per spectroscopic technique was developed
139 (table 1). The UV calibration model of the gel was developed applying mean-centering,
140 Standard Normal Variate (SNV) correction and first-derivative transformation as
141 preprocessing methods in combination with selecting the spectral region between 280 -
142 297 nm (table 1). The Raman spectra of the gel were mean-centered and SNV corrected,
143 followed by taking the first derivative and selecting the spectral regions where the API
144 showed Raman activity. SNV preprocessing was applied to eliminate baseline offset
145 variations, which can be caused by scatter differences between the samples. First
146 derivative transformation allowed a better visualization of small absorption bands and
147 corrected for baseline shifts [33].

148 The API concentrations (Y) were regressed against the corresponding in-line collected
149 preprocessed spectra (X) through a PLS method. The goodness of fit and the predictive
150 ability of the developed PLS models were assessed by the calculation of R^2 and Q^2 ,
151 respectively. Q^2 values were obtained after performing a leave-one-out cross-validation,
152 in which sub-models were developed from a reduced calibration dataset and the excluded
153 data was predicted by the sub-models. The number of PLS components providing the
154 highest Q^2 value was selected. Details of the developed UV and Raman PLS models of
155 the suspension are also displayed in table 1. The PLS models were created using the
156 SIMCA software (Version 14, Umetrics, Umeå, Sweden).

157 **2.2.6. Validation of the calibration models**

158 The predictive properties of the developed models were first assessed by computation of
159 the Root Mean Square Error of Prediction (RMSEP), obtained when predicting the
160 external validation sets. During validation, the within-day, between-day and operator
161 variability were incorporated. Accuracy profiles were adopted to evaluate the validation of
162 the developed analytical methods and are proposed by SFSTP as a harmonized approach
163 for the validation of quantitative analytical procedures [30]–[32]. The objective of validation
164 is to ensure that the difference between the measured value (x_i) and the unknown true
165 value of the sample (μ_T) will be lower than an acceptance limit (λ):

$$166 \quad |x_i - \mu_T| < \lambda \quad (1)$$

167 Here, λ was set at 10 %. For an analytical method to be considered as acceptable, it must
168 be assured that the probability that a measurement will fall outside the acceptance limits
169 is less than or equal to the maximum risk that the analyst is able to take during routine
170 use:

$$171 \quad \Pr(|x_i - \mu_T| < \lambda) \geq \beta \quad (2)$$

172 The desired proportion of measurements inside the acceptance limits (β) was set at 95
173 %. The computation of a large number of validation parameters (e.g., precision, trueness,
174 linearity, ...) is not sufficient to decide whether the objectives of validation are ensured.
175 Therefore, the accuracy profile was used as a decision tool for the validity of the analytical
176 methods, which is constructed from the total error of the method, being the sum of the
177 random error (precision) and systematic error (trueness) [32]. For the precision, both the

178 repeatability (within-day variability) and intermediate precision (between-day and operator
179 variability) were calculated [34]. In the accuracy profiles, the acceptance limits are plotted
180 together with the relative error of the individual predictions, the relative bias and the β -
181 expectation tolerance intervals at each concentration level of the validation set. Here, the
182 acceptance limits were set at 10 % relative error. The β -expectation tolerance intervals
183 visualise at each concentration level where at least 95 out of 100 future measurements
184 given by the analytical procedure will fall between [35]. The intersect between the
185 acceptance limits and the β -expectation tolerance intervals defines the upper and lower
186 quantification limits of the analytical method. The accuracy profiles were calculated from
187 the data obtained from the validation experiments.

188 Furthermore, the standard deviation of the β -expectation tolerance intervals was used for
189 the estimation of the standard uncertainty in the measurements [36]. The uncertainty is
190 defined as a parameter associated with the result of a measurement, that characterises
191 the dispersion of the values that could reasonably be attributed to the measurand. The
192 measurement uncertainty was expressed by four uncertainty parameters: uncertainty of
193 the bias, uncertainty (combination of uncertainty of the bias with the intermediate precision
194 standard deviation), expanded uncertainty and the relative expanded uncertainty. The
195 expanded uncertainty represents an interval around the mean value where the unknown
196 true value can be located with a certain confidence level (here 95 %). The relative
197 expanded uncertainty is calculated as the expanded uncertainty divided by the
198 corresponding true concentration [37].

199 **3. RESULTS AND DISCUSSION**

200 The development and validation of the PLS models for the gel formulation, based on the
201 measurements with the two spectroscopic techniques (UV and Raman spectroscopy), will
202 be discussed in detail in the results section. Information regarding the development and
203 validation of the PLS models of the suspension can be found in tables 1, 2, 3 and 4.

204 **3.1. Development of the calibration models**

205 **3.1.1. UV spectroscopy**

206 The in-line UV/VIS measurements were made in the 200 - 1100 nm spectral range. Only
207 the UV region (200 - 400 nm) was investigated, since the size of the conjugated system
208 of the API was not large enough to absorb in the VIS region [38]. Also, prominent
209 deuterium peaks were present in the VIS region (486 and 656 nm), which were not of
210 interest [39]. In a first step, the molecular structure of the API in the gel was screened for
211 UV activity. Several aromatic groups were found in the molecular structure and suggested
212 that the API will absorb in the UV region. The exact absorption wavelength is dependent
213 of the type and number of functional groups coupled to the aromatic rings, which can shift
214 the absorption wavelength to lower or higher wavelengths [38]. To confirm whether the
215 API could indeed be detected in the UV spectra of the gel, where possible interfering
216 components are present, the spectra of the calibration batch were coloured according to
217 concentration level and it was checked whether the colours were in sequence with the
218 concentration levels. A distinctive peak in the region 280 - 297 nm was observed in the
219 SNV-corrected and first-derived UV spectra of the gel, where the spectra were clearly
220 clustered according to API concentration (figure 2).

221 A PLS model was developed from the mean-centered, SNV-corrected and first-derived
222 UV spectra of the gel between 280 - 297 nm ($R^2 = 0.988$; $Q^2 = 0.988$; Root Mean Square
223 Error of Cross Validation (RMSECV) = 0.0274 % w/w) (table 1 and 2). Selecting this
224 spectral region eliminated interfering variance sources, thereby increasing the variance
225 due to concentration differences. RMSEP values (0.0584, 0.0709 and 0.0588 % w/w) of
226 the gel were calculated from the predictions of the three validation batches. Also for the
227 suspension a calibration model was developed, following the same strategy as described
228 for the gel (table 1 and 2).

229 **3.1.2. Raman spectroscopy**

230 The Raman spectra of the gel formulation (calibration batch) and pure API are presented
231 in figure 3. The peaks in the spectra of the pure API with the highest intensity are situated
232 around 396, 660, 1348 and 1590 cm^{-1} . It can be noticed from figure 3 that at these Raman
233 shifts, peaks in the spectra of the gel are visible. A detail of the preprocessed spectra of
234 the gel calibration set at the above mentioned spectral regions is shown in figure 4.
235 Applying these preprocessing methods highlighted the spectral differences most. A logic
236 concentration trend in the spectra was observed at the API selective bands: increasing
237 Raman intensity for an increasing API concentration. These four regions were the most
238 abundant peaks in the Raman spectra of the pure API (figure 3), suggesting that the trend
239 in the spectra was caused by the difference in API concentration.

240 The model of the gel formulation with the highest predictive performance ($R^2 = 0.973$; Q^2
241 = 0.973; RMSECV = 0.0418 % w/w) was created from the mean-centered, SNV corrected
242 and first-derived Raman spectra in the regions 390 - 405, 655 - 667, 1340 - 1355 and

243 1570 - 1600 cm^{-1} (table 1). The selection of these spectral regions was based on the
244 evaluation of the Raman spectra of the pure API and gel (figure 3 and 4). The resulting
245 RMSEP values of the three validation sets were 0.0255, 0.0235 and 0.0381 % (w/w). The
246 PLS model of the suspension, measured with the Raman PhAT probe, was constructed
247 using the same strategy as described above and detailed information regarding the
248 construction of the model together with the resulting RMSECV and RMSEP values can
249 be found in table 1 and 2.

250 **3.2. Validation of the calibration models**

251 **3.2.1. UV spectroscopy**

252 **3.2.1. UV spectroscopy**

253 The accuracy profile for the UV-based in-line quantification method of the gel is displayed
254 in figure 5a. At each validation concentration level, the β -expectation tolerance intervals
255 exceeded the acceptance limits (10 % relative error) (figure 5a). Furthermore, the
256 predictions of the lowest API concentration level (1.75 % w/w) were more biased than the
257 other concentration levels (table 3). This is probably because of the difficulty to detect this
258 low API concentration. The calculated precision parameters (repeatability and
259 intermediate precision) from the UV-based in-line quantification method showed that the
260 intermediate precision Relative Standard Deviation (RSD) was much higher compared to
261 the repeatability RSD at all concentration levels (table 3). Because of the lower
262 intermediate precision, an important day or operator effect was causing variability in the
263 predictions.

264 The accuracy profile of the UV-based in-line quantification method of the suspension is
265 displayed in figure 6a. Between the API concentration range of 0.0865 - 0.0955 % (w/w),

266 the β -expectation tolerance intervals fell within the acceptance limits of 10 % (relative
267 error). Therefore, future measurements between an API concentration of 0.0865 and
268 0.0955 % (w/w) obtained by this procedure have a probability of 95 % that the difference
269 between the measured concentration and the true concentration is less than 10 % (relative
270 error). However, the β -expectation tolerance intervals at the lowest (0.0774 % w/w) and
271 highest (0.1046 % w/w) API concentration level were almost exceeding the 20 % (relative
272 error) acceptance limits. The relative bias at API concentration level 0.0774 and 0.1046
273 % (w/w) was 3.04 and -4.05 %, respectively. This value is remarkably higher than the
274 relative bias (1.40, 0.65 and -0.92 %) of the other validation concentration levels.
275 Furthermore, a higher imprecision for the lowest and highest concentration level was
276 observed, which was mainly induced by a low intermediate precision, suggesting an
277 important day or operator effect. Table 2 shows that the RMSEP of day 1 (0.00496 % w/w)
278 was almost four times higher than the RMSEP of day 2 (0.00148 % w/w) and 3 (0.00171
279 % w/w). A cause for the less accurate predictions of the day 1 validation samples was not
280 found, but could be operator related such as an accidental alteration in the production
281 process of these validation samples.

282 **3.2.2. Raman spectroscopy**

283 For the accuracy profile of the Raman-based in-line quantification method of the gel, the
284 β -expectation tolerance intervals exceeded the 10 % (relative error) acceptance limits only
285 at the 1.75 % (w/w) API concentration level (figure 5b). Hence, in the 1.96 - 2.37 % (w/w)
286 API concentration range, 95 out of 100 future measurements will be included within the
287 acceptance limits of 10 % (relative error) and even within the 5 % (relative error)
288 acceptance limits, when using this analytical method. To explain the large β -expectation

289 tolerance interval at the 1.75 % (w/w) API concentration level, the trueness and precision
290 were investigated. The calculated relative bias and RSD for repeatability at this level were
291 not higher than for the other concentration levels, but the intermediate precision RSD was
292 higher (table 3). There was indeed one validation batch (day 3) where the predictions of
293 the lowest concentration level were lower in comparison to the other validation batches.
294 This variability could be caused by the detection sensitivity limitations of the Raman
295 method at the lowest concentration level.

296 The accuracy profile for the in-line Raman-based quantification method of the suspension
297 was developed following the same strategy as described above and is displayed in figure
298 6b. The β -expectation tolerance intervals exceeded the 10 % (relative error) acceptance
299 limits over the whole concentration range, except for the API concentration levels 0.0862
300 and 0.0953 % (w/w). The accuracy profile has a clear downward trend, i.e., low
301 concentration levels were predicted higher, the intermediate concentration level was
302 predicted around the target concentration and the high concentration levels were
303 predicted lower. This demonstrated that all the concentration levels were predicted as the
304 same value, indicating that the small changes in API concentration could not be detected
305 and that the quantification of the low-dosed API in this suspension could not be achieved
306 with Raman spectroscopy.

307 When the accuracy profiles and validation parameters of the UV and Raman quantification
308 methods of the suspension are compared, it is clear that the in-line quantification of the
309 API only was possible with UV spectroscopy (table 2 and 3). To better understand the
310 difference in predictive performance of both spectroscopic techniques, the in-line UV and
311 Raman spectra of the suspension calibration set were investigated (figure 7). The UV

312 spectra are clearly separated according to API concentration between 310 - 325 nm,
313 which confirmed the quantification ability and high sensitivity of UV spectroscopy for this
314 API. In the Raman spectra, no spectral differences between the concentration levels are
315 seen and no API specific peaks can be located in the spectra of the suspension, despite
316 investigating a region of the spectra where the API is Raman active. Increasing the
317 exposure time and number of scans of the Raman spectrometer had no impact on the
318 detection of the API.

319 The high sensitivity of UV spectroscopy was correlated with the strong UV activity of the
320 API in the suspension, due to conjugated double bonds in its molecular structure [38],
321 [40]. However, the molecular structure of the API also meets to the requirements (non-
322 polar bonds and aromatic rings) for good Raman activity, suggesting that the failure of the
323 Raman method for the suspension is linked to the inherent weak Raman effect [17], [41].
324 Raman spectroscopy applies monochromatic light to irradiate the samples and the
325 incident light is scattered by the sample molecules. Most of this light is scattered at the
326 same frequency, i.e., Raleigh radiation. Only one in 10^8 incident photons is scattered with
327 a different frequency than the incident light (Raman effect). This in combination with the
328 small fraction of light which is scattered into the same direction of the probe, explains why
329 the quantification of low concentrations can be an issue for Raman spectroscopy [41].

330 UV spectroscopy was identified as a novel and alternative in-line spectroscopic tool for
331 quantification purposes, in addition to the widely used Raman spectroscopy. Important is
332 that none of the two spectroscopic techniques was superior to the other for both the
333 formulations. While Raman was more accurate in quantifying the API in the gel (2 % w/w),
334 the in-line UV-based method for the suspension performed better than the in-line Raman-

335 based method. This study illustrated that spectroscopic techniques can be complementary
336 and that the preferred technique is dependent on several factors such as the molecular
337 structure of the API, concentration of the analyte, measurement conditions, presence of
338 interfering components, measurement time and cost. In addition, the UV immersion probe
339 was more practical to work with inside a process environment, because the probe tip can
340 be in direct contact with the sample. Furthermore, UV spectroscopy is a suitable PAT-tool
341 for measurements in aqueous environments, since the suspension contained water. This
342 would be challenging for NIR spectroscopy because water creates strong absorbance
343 peaks in the near infrared region, which can potentially overwhelm the signal(s) of the API
344 [41]. Preliminary off-line experiments with NIR spectroscopy showed that the APIs had
345 weak signals in the near infrared region and therefore NIR spectroscopy was not further
346 investigated in this study.

347 The measurement uncertainty of the UV- and Raman-based calibration models is
348 summarized in table 4 in terms of the uncertainty of the bias, uncertainty, expanded
349 uncertainty and the relative expanded uncertainty at each concentration level of the
350 validation sets [36]. For the UV-based method of the suspension, the relative expanded
351 uncertainty at the target API concentration (0.09 % w/w) was 3.82 % (relative error) (table
352 4). This means that the unknown true value is located at a maximum of ± 3.82 % (relative
353 error) around the measured value, with a confidence level of 95 %. In comparison, the
354 relative expanded uncertainty at the target concentration of the suspension was 6.53 %
355 (relative error) for the Raman-based method.

356 **4. CONCLUSIONS**

357 In this study, analytical methods based on in-line UV spectroscopy were developed for
358 the quantification of APIs in pharmaceutical semi-solid and liquid formulations. The
359 performance of this new PAT-tool was compared with an already more established PAT-
360 method based on Raman spectroscopy. In-line UV measurements were carried out with
361 an immersion probe while for the Raman measurements a PhAT probe was used. The
362 validation of the analytical methods was evaluated by the calculation of accuracy profiles,
363 ensuring that 95 out of 100 future routine measurements will be included within the present
364 acceptance limits of 10 % (relative error). Furthermore, the uncertainty of bias and the
365 expanded uncertainty were estimated at each concentration level. The results show that
366 the calibration model developed from the Raman PhAT probe data had a higher accuracy
367 than the UV-based model for the gel formulation (2 % (w/w) API). The UV method
368 developed for the low-dosed suspension (0.09 % (w/w) API) had good performance
369 characteristics, whereas the quantification of this low concentration was not possible with
370 Raman spectroscopy due to detection sensitivity limitations. It was demonstrated that UV
371 spectroscopy can be adopted as a novel PAT-tool for in-line and real-time quantification
372 purposes during the manufacturing of pharmaceutical semi-solid and liquid formulations
373 and that it can be complementary to other spectroscopic techniques, especially when the
374 detection sensitivity is not sufficient. However, the feasibility of the spectroscopic
375 technique is case dependent and should therefore be assessed in preliminary feasibility
376 studies.

377 **FUNDING**

378 Research funded by a PhD grant of the Research Foundation Flanders (FWO).

REFERENCES

- [1] Y. Roggo, K. Degardin, and P. Margot, "Identification of pharmaceutical tablets by Raman spectroscopy and chemometrics," *Talanta*, vol. 81, no. 3, pp. 988–995, 2010.
- [2] S. Romero-Torres, J. D. Pérez-Ramos, K. R. Morris, and E. R. Grant, "Raman spectroscopic measurement of tablet-to-tablet coating variability," *J. Pharm. Biomed. Anal.*, vol. 38, no. 2, pp. 270–274, 2005.
- [3] T. R. M. De Beer, C. Bodson, B. Dejaegher, B. Walczak, P. Vercruyse, A. Burggraeve, A. Lemos, L. Delattre, Y. Vander Heyden, J. P. Remon, C. Vervaet, and W. R. G. Baeyens, "Raman spectroscopy as a process analytical technology (PAT) tool for the in-line monitoring and understanding of a powder blending process," *J. Pharm. Biomed. Anal.*, vol. 48, no. 3, pp. 772–779, 2008.
- [4] D. S. Hausman, R. T. Cambron, and A. Sakr, "Application of Raman spectroscopy for on-line monitoring of low dose blend uniformity," *Int. J. Pharm.*, vol. 298, no. 1, pp. 80–90, 2005.
- [5] I. Lewis and L. S. Taylor, "spectroscopic techniques Comparison of Sampling Techniques for In-Line Monitoring Using Raman Spectroscopy," *Appl. Spectrosc.*, vol. 59, no. 7, 2005.
- [6] G. J. Vergote, T. R. M. De Beer, C. Vervaet, J. P. Remon, W. R. G. Baeyens, N. Dierick, and F. Verpoort, "In-line monitoring of a pharmaceutical blending process using FT-Raman spectroscopy," *Eur. J. Pharm. Sci.*, vol. 21, no. 4, pp. 479–485, 2004.
- [7] L. Saerens, L. Dierickx, B. Lenain, C. Vervaet, J. P. Remon, and T. De Beer, "Raman spectroscopy for the in-line polymer-drug quantification and solid state characterization during a pharmaceutical hot-melt extrusion process," *Eur. J. Pharm. Biopharm.*, vol. 77, no. 1, pp. 158–163, 2011.
- [8] P. D. Coates, S. E. Barnes, M. G. Sibley, E. C. Brown, H. G. M. Edwards, and I. J. Scowen, "In-process vibrational spectroscopy and ultrasound measurements in polymer melt extrusion," *Polymer (Guildf.)*, vol. 44, no. 19, pp. 5937–5949, 2003.
- [9] S. Barnes and M. Sibley, "Process monitoring of polymer melts using in-line spectroscopy," *Trans. Inst. Meas. Control*, vol. 5, pp. 453–465, 2007.
- [10] T. R. M. De Beer, W. R. G. Baeyens, A. Vermeire, D. Broes, J. P. Remon, and C. Vervaet, "Raman spectroscopic method for the determination of medroxyprogesterone acetate in a pharmaceutical suspension: validation of quantifying abilities, uncertainty assessment and comparison with the high performance liquid chromatography reference method," *Anal. Chim. Acta*, vol. 589, no. 2, pp. 192–199, 2007.
- [11] S. C. Park, M. Kim, J. Noh, H. Chung, Y. Woo, J. Lee, and M. S. Kemper, "Reliable and fast quantitative analysis of active ingredient in pharmaceutical suspension using Raman spectroscopy," *Anal. Chim. Acta*, vol. 593, no. 1, pp. 46–53, 2007.
- [12] M. Kim, H. Chung, Y. Woo, and M. S. Kemper, "A new non-invasive, quantitative Raman technique for the determination of an active ingredient in pharmaceutical liquids by direct measurement through a plastic bottle," *Anal. Chim. Acta*, vol. 587, no. 2, pp. 200–207, 2007.
- [13] B. Gotter, W. Faubel, S. Heißler, J. Hein, and R. Neubert, "Determination of drug content in semisolid formulations by non-invasive spectroscopic methods: FTIR-ATR, -PAS, -Raman and PDS," *J. Phys. Conf. Ser.*, vol. 214, p. 12129, 2010.
- [14] T. R. M. De Beer, W. R. G. Baeyens, Y. Vander Heyden, J. P. Remon, C. Vervaet, and F. Verpoort, "Influence of particle size on the quantitative determination of salicylic acid in a pharmaceutical ointment using FT-Raman spectroscopy," *Eur. J. Pharm. Sci.*, vol. 30, no. 3–4, pp. 229–235, 2007.
- [15] M. T. Islam, Rodriguez-Hornedo, S. Ciotti, and C. Ackermann, "The potential of Raman spectroscopy as a process analytical technique during formulations of topical gels and emulsions," *Pharm. Res.*, vol. 21, no. 10, pp. 1844–1851, 2004.
- [16] T. R. M. De Beer, W. R. G. Baeyens, J. Ouyang, C. Vervaet, and J. P. Remon, "Raman spectroscopy as a process analytical technology tool for the understanding and the quantitative in-line monitoring of the homogenization process of a pharmaceutical suspension," *R. Soc. Chem.*, vol. 131, pp. 1137–1144, 2006.
- [17] K. A. Bakeev, *Process Analytical Technology – Second Edition*. 2010.
- [18] S. Warnecke, A. Rinnan, M. Allesø, and S. B. Engelsen, "Fluorescence Spectroscopy in Process Analytical Technology (PAT): Simultaneous Quantification of Two Active Pharmaceutical Ingredients in a Tablet Formulation," *Appl. Spectrosc.*, vol. 69, no. 3, pp. 323–331, 2015.
- [19] N. Shanker and S. L. Bane, "Basic Aspects of Absorption and Fluorescence Spectroscopy and Resonance Energy Transfer Methods," *Methods Cell Biol.*, vol. 84, no. 7, pp. 213–242, 2008.
- [20] J. J. Moes, M. M. Ruijken, E. Gout, H. W. Frijlink, and M. I. Ugwoke, "Application of process analytical technology in tablet process development using NIR spectroscopy: Blend uniformity, content uniformity and coating thickness measurements," *Int. J. Pharm.*, vol. 357, no. 1–2, pp. 108–118, 2008.
- [21] G. M. Hadad, A. El-Gindy, and W. M. M. Mahmoud, "HPLC and chemometrics-assisted UV-spectroscopy methods for the simultaneous determination of ambroxol and doxycycline in capsule," *Spectrochim. Acta - Part A Mol. Biomol. Spectrosc.*, vol. 70, no. 3, pp. 655–663, 2008.
- [22] D. Bonazzi, R. Gotti, V. Andrisano, and V. Cavrini, "Analysis of ACE inhibitors in pharmaceutical dosage forms by derivative UV spectroscopy and liquid chromatography (HPLC)," *J. Pharm. Biomed. Anal.*, vol. 16, no. 3, pp. 431–438, 1997.
- [23] M. Sumithra, P. Shanmugasundaram, and K. Srinivasulu, "Analytical method development and validation of lafutidine in tablet dosage form by RP-HPLC," *Int. J. ChemTech Res.*, vol. 3, no. 3, pp. 1403–1407, 2011.
- [24] K. Nie, L. Li, X. Li, Y. Zhang, X. Mu, and J. Chen, "Sustained-Release Tablets Release by Test System," *Dissolution Technol.*, no. February, pp. 16–19, 2009.
- [25] S. O. Keeffe, C. Fitzpatrick, and E. Lewis, "An optical fibre based ultra violet and visible absorption spectroscopy system for ozone concentration monitoring," *Sensors and Actuators*, vol. 125, pp. 372–378, 2007.
- [26] A. C. Quinn, P. J. Gemperline, B. Baker, M. Zhu, and D. S. Walker, "Fiber-optic UV/visible composition monitoring for process control of batch reactions," *Chemom. Intell. Lab. Syst.*, vol. 45, pp. 199–214, 1999.
- [27] D. J. W. Ng and M. Ā. Assirelli, "MIXING STUDY IN BATCH STIRRED VESSELS USING A FIBRE-OPTIC UV-VIS MONITORING TECHNIQUE,"

- Chem. Eng. Res. Des.*, vol. 85, no. 1995, pp. 1348–1354, 2007.
- [28] X. Lu, R. Lozano, and P. Shah, "In-Situ Dissolution Testing Using Different UV Fiber Optic Probes and Instruments," *Dissolution Technol.*, pp. 6–15, 2003.
- [29] J. Müller, K. Knop, J. Thies, C. Uerpmann, and P. Kleinebudde, "Feasibility of Raman spectroscopy as PAT tool in active coating.," *Drug Dev. Ind. Pharm.*, vol. 36, no. 2, pp. 234–243, 2010.
- [30] P. Hubert, J. J. Nguyen-Huu, B. Boulanger, E. Chapuzet, P. Chiap, N. Cohen, P. A. Compagnon, W. Dewé, M. Feinberg, M. Lallier, M. Laurentie, N. Mercier, G. Muzard, C. Nivet, and L. Valat, "Harmonization of strategies for the validation of quantitative analytical procedures A SFSTP proposal—part I," *J. Pharm. Biomed. Anal.*, vol. 36, no. 3, pp. 579–586, 2004.
- [31] N. C. Ph. Hubert a, J.-J. Nguyen-Huub, B. Boulanger c, E. Chapuzet d, P. Chiap e, M. L. k P.-A. Compagnong, W. Dewé, M. Feinberg i, M. Lallier j, and E. R. a N. Mercier d, G. Muzardl, C. Nivetm, L. Valat n, "Harmonization of strategies for the validation of quantitative analytical procedures A SFSTP proposal – Part II," *J. Pharm. Biomed. Anal.*, vol. 45, pp. 70–81, 2007.
- [32] P.-A. C. Ph. Hubert a, J.-J. Nguyen-Huub, B. Boulanger c, E. Chapuzet d, N. Cohene and E. R. a W. Dewé g, M. Feinberg h, M. Laurentie i, N. Mercier d, G. Muzardj, L. Valat k, "Harmonization of strategies for the validation of quantitative analytical procedures A SFSTP proposal—Part III," *J. Pharm. Biomed. Anal.*, vol. 45, pp. 82–96, 2007.
- [33] J. Luypaert, S. Heuerding, Y. Vander Heyden, and D. L. Massart, "The effect of preprocessing methods in reducing interfering variability from near-infrared measurements of creams," *J. Pharm. Biomed. Anal.*, vol. 36, pp. 495–503, 2004.
- [34] International Conference on Harmonisation of Technical Requirements for Registration of Pharmaceuticals for Human use, "VALIDATION OF ANALYTICAL PROCEDURES: TEXT AND METHODOLOGY Q2 (R1)," 2015.
- [35] R. Mee, "β-Expectation and β-Content Tolerance Limits for Balanced One-Way ANOVA Random Model," *Technometrics*, vol. 26, no. 3, pp. 251–254, 1984.
- [36] M. Feinberg, B. Boulanger, W. Dewé, and P. Hubert, "New advances in method validation and measurement uncertainty aimed at improving the quality of chemical data," *Anal. Bioanal. Chem.*, vol. 380, no. 3 SPEC.ISS., pp. 502–514, 2004.
- [37] Eurachem/CITAC Guide CG 4, *Quantifying Uncertainty in Analytical Measurement Third Edition*. 2012.
- [38] D. G. Watson, *Pharmaceutical analysis: a textbook for pharmacy students and pharmaceutical chemists*. 1999.
- [39] B. M. Ham and A. MaHam, *Analytical Chemistry: A Chemist and Laboratory Technician's Toolkit*. 2015.
- [40] R. M. Silverstein, *Spectrometric Identification of Organic Compounds*, 6th ed. New York: John Wiley & Sons, 1998.
- [41] T. De Beer, A. Burggraave, M. Fonteyne, L. Saerens, J. P. Remon, and C. Vervaet, "Near infrared and Raman spectroscopy for the in-process monitoring of pharmaceutical production processes," *Int. J. Pharm.*, vol. 417, no. 1–2, pp. 32–47, 2011.

	Gel (2 % w/w)		Suspension (0.09 % w/w)	
	UV	Raman	UV	Raman
Exposure time (s)	1	15	0.95	15
Scans	5	1	5	1
Preprocessing methods	Mean-centering SNV 1 st derivative	Mean-centering SNV 1 st derivative	Mean-centering 1 st derivative	Mean-centering SNV 1 st derivative
Spectral region (UV: nm, Raman: cm ⁻¹)	280.1-296.9	390.1-404.8 655.0-666.7 1340.2-1354.9 1570.0-1600.0	310.1-325.6	1390.0-1430.2
R ²	0.988	0.973	0.995	0.115
Q ²	0.988	0.973	0.995	0.028
# of PLS components	2	1	2	1

Table 1. Exposure time, number of scans, preprocessing methods, spectral region(s), R², Q² and number of PLS components of the developed calibration models.

	Gel (2 % w/w)		Suspension (0.09 % w/w)	
	UV	Raman	UV	Raman
RMSECV (% w/w)	0.0274	0.0418	0.000819	0.0108
RMSEP day 1 (% w/w)	0.0584	0.0255	0.00496	0.00947
RMSEP day 2 (% w/w)	0.0709	0.0235	0.00148	0.00996
RMSEP day 3 (% w/w)	0.0588	0.0381	0.00171	0.00951

Table 2. RMSECV and RMSEP values of the UV and Raman calibration models for each formulation.

Spectroscopic technique	Concentration level (% w/w)	Relative bias (%)	Repeatability (RSD, %)	Intermediate precision (RSD, %)	Relative B-expectation tolerance limits (%)
Gel (2 % w/w)					
UV	1.75	-3.02	1.239	2.341	-11.14;5.10
	1.96	-0.88	0.838	2.652	-13.82;12.05
	2.06	-0.01	0.496	2.465	-12.21;12.19
	2.16	0.12	1.869	3.277	-11.56;11.80
	2.37	-1.05	1.040	2.226	-11.77;9.66
Raman	1.75	0.17	0.815	2.097	-10.12;10.46
	1.96	-0.48	1.127	1.225	-3.46;2.49
	2.06	-1.13	0.881	0.944	-3.36;1.10
	2.16	-0.97	0.627	0.815	-3.23;1.29
	2.37	-0.89	0.726	1.051	-4.07;2.30
Suspension (0.09 % w/w)					
UV	0.0774	3.04	0.752	4.479	-19.83;25.91
	0.0865	1.40	0.411	1.376	-5.47;8.28
	0.0910	0.65	0.417	1.653	-7.57;8.86
	0.0955	-0.92	0.508	1.848	-9.95;8.11
	0.1046	-4.05	0.785	4.501	-25.44;17.35
Raman	0.0772	16.06	2.425	3.035	6.72;25.40
	0.0862	4.90	1.437	1.437	1.40;8.40
	0.0908	0.28	1.653	2.910	-10.11;10.67
	0.0953	-4.08	2.429	2.429	-9.49;1.32
	0.1044	-12.65	2.744	2.744	-18.21;-7.09

Table 3. In-line UV and Raman quantification methods: validation parameters per concentration level for the gel and suspension.

Spectroscopic technique	Concentration level (% w/w)	Uncertainty of the bias (% w/w)	Uncertainty (% w/w)	Expanded uncertainty (% w/w)	Relative expanded uncertainty (%)
Gel (2 % w/w)					
UV	1.75	0.0204	0.0447	0.0894	5.10
	1.96	0.0286	0.0588	0.1177	6.01
	2.06	0.0289	0.0584	0.1168	5.67
	2.16	0.0356	0.0794	0.1588	7.34
	2.37	0.0275	0.0590	0.1180	4.98
Raman	1.75	0.0200	0.0418	0.0837	4.78
	1.96	0.0083	0.0252	0.0505	2.58
	2.06	0.0065	0.0203	0.0405	1.97
	2.16	0.0075	0.0190	0.0380	1.76
	2.37	0.0114	0.0271	0.0543	2.29
Suspension (0.09 % w/w)					
UV	0.0774	0.0020	0.0041	0.0082	10.63
	0.0865	0.0007	0.0014	0.0028	3.20
	0.0910	0.0009	0.0017	0.0035	3.82
	0.0955	0.0010	0.0020	0.0040	4.20
	0.1046	0.0026	0.0052	0.0104	9.94
Raman	0.0772	0.0011	0.0029	0.0059	7.63
	0.0862	0.0004	0.0014	0.0027	3.14
	0.0908	0.0013	0.0030	0.0059	6.53
	0.0953	0.0006	0.0023	0.0046	4.85
	0.1044	0.0007	0.0026	0.0052	4.99

Table 4. In-line UV and Raman quantification methods: estimates of the measurement uncertainties on the API concentration at each concentration level per formulation.



Figure 1. Experimental setup: (a) customized mixing system without probes; (b) UV immersion probe; (c) Raman PhAT probe.

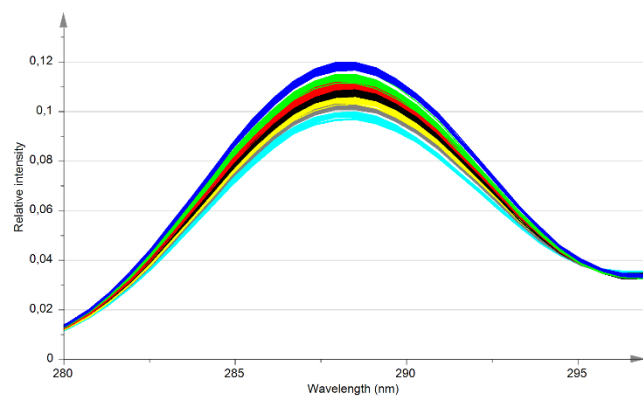


Figure 2. In-line UV spectra of the gel calibration batch between 280 - 300 nm (SNV and first derivative). Turquoise: 80 %, grey: 90 %, yellow: 95 %, black: 100 %, red: 105 %, green: 110 %, blue: 120 %.

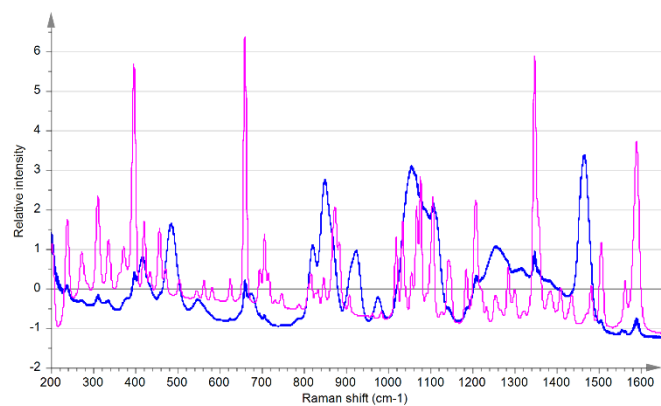


Figure 3. In-line Raman spectra (SNV) of the gel calibration batch (blue) and off-line spectra of the pure API (pink).

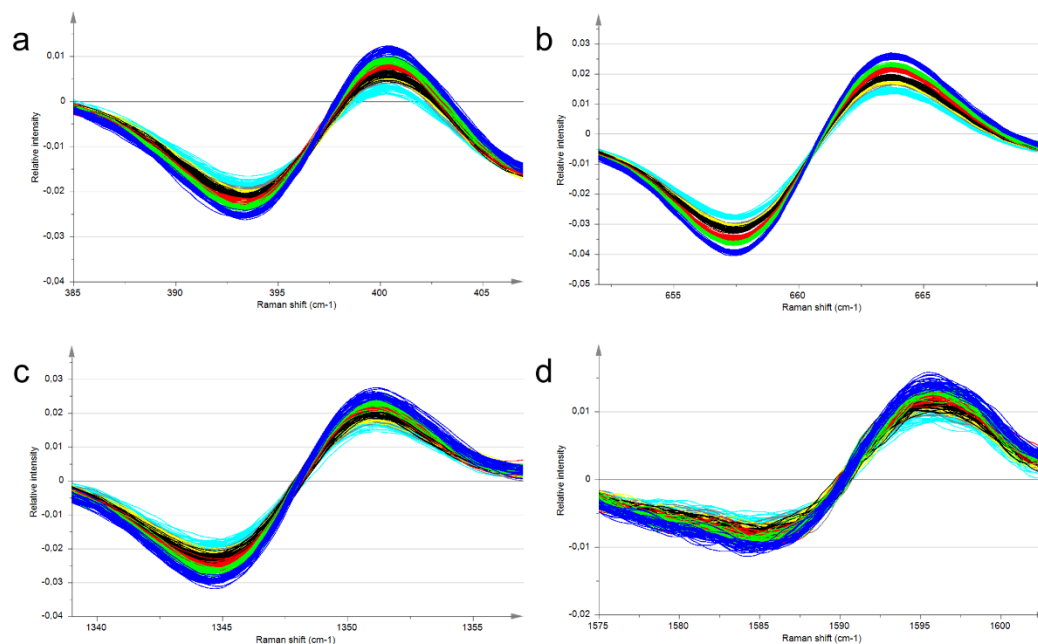


Figure 4. Detail of in-line Raman spectra (SNV and first derivative) of the gel calibration batch at the following spectral regions : (a) 385 – 407 cm^{-1} , (b) 652 – 669 cm^{-1} , (c) 1339 – 1357 cm^{-1} and (d) 1575 – 1602 cm^{-1} . Turquoise: 80 %, grey: 90 %, yellow: 95 %, black: 100 %, red: 105 %, green: 110 %, blue: 120 %.

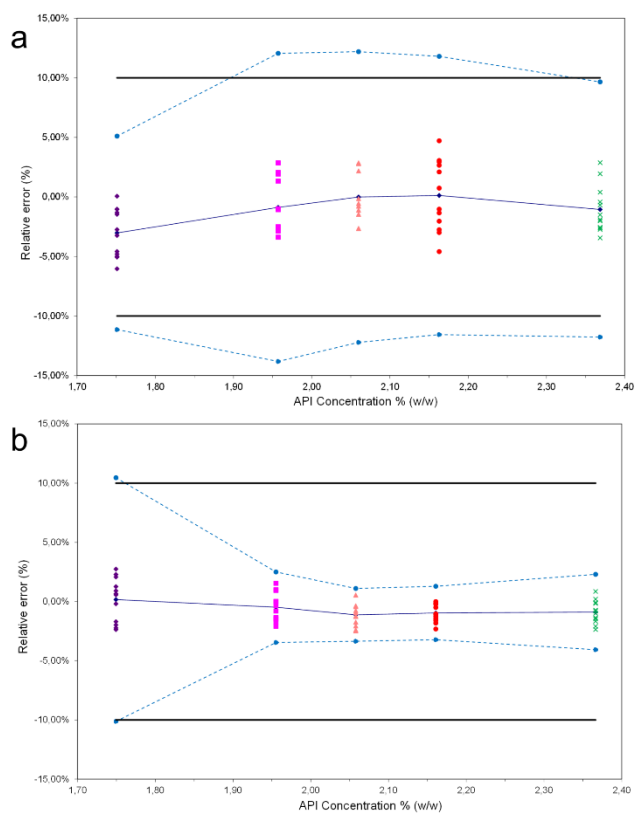


Figure 5. Accuracy profiles of the (a) UV and (b) Raman in-line quantification methods for the gel. Plain black lines: acceptance limits set at 10 % (relative error), dashed blue lines: β -expectation tolerance limits, plain blue line: relative bias.

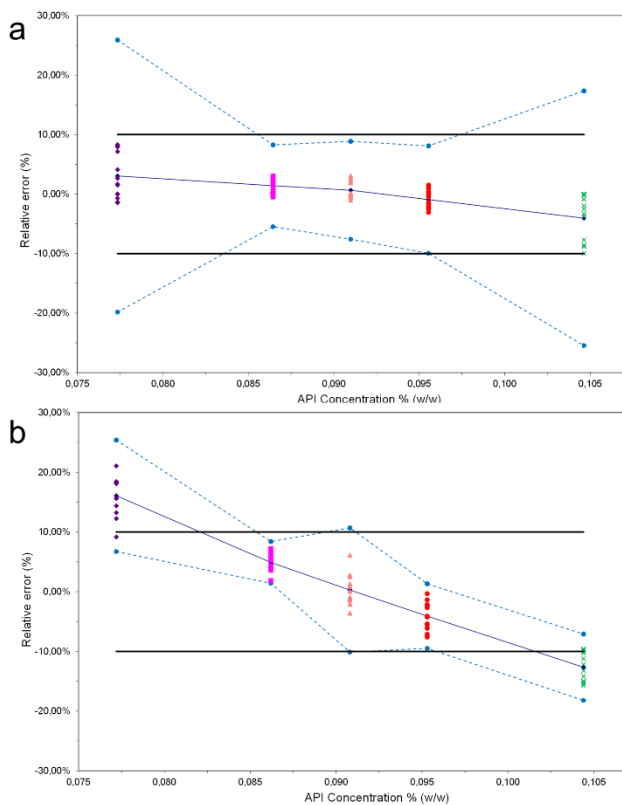


Figure 6. Accuracy profiles of the (a) UV and (b) Raman in-line quantification methods for the suspension. Plain black lines: acceptance limits set at 10 % (relative error), dashed blue lines: β -expectation tolerance limits, plain blue line: relative bias.

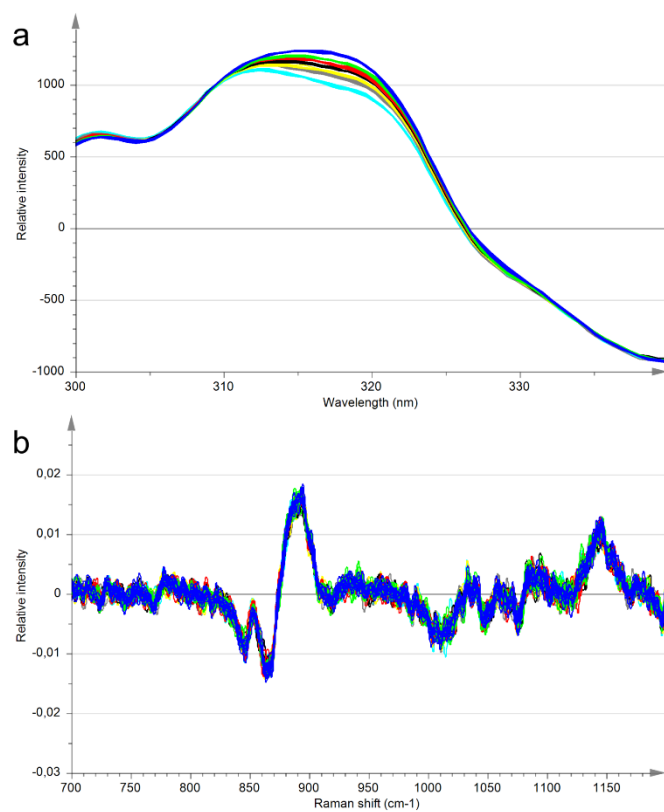


Figure 7. Preprocessed in-line (a) UV and (b) Raman spectra of the suspension calibration batch. Turquoise: 80 %, grey: 90 %, yellow: 95 %, black: 100 %, red: 105 %, green: 110 %, blue: 120 %.